Reduction of electron deficient guanine radical species in plasmid DNA by tyrosine derivatives

Mandi Tsoi, Trinh T. Do, Vicky J. Tang, Joseph A. Aguilera and Jamie R. Milligan*

Received 30th October 2009, Accepted 12th March 2010
First published as an Advance Article on the web 24th March 2010
DOI: 10.1039/b922749k

Guanine bases are the most easily oxidized sites in DNA and therefore electron deficient guanine radical species are major intermediates in the direct effect of ionizing radiation (ionization of the DNA itself) on DNA as a consequence of hole migration to guanine. As a model for this process we have used gamma-irradiation in the presence of thiocyanate ions to generate single electron oxidized guanine radicals in a plasmid target in aqueous solution. The stable species formed from these radicals can be detected and quantified by the formation of strand breaks in the plasmid after a post-irradiation incubation using a suitable enzyme. If a tyrosine derivative is also present during irradiation, the production of guanine oxidation products is decreased by electron transfer from tyrosine to the intermediate guanyl radical species. By using cationic tyrosine containing ligands we are able to observe this process when the tyrosine is electrostatically bound to the plasmid. The driving force dependence of this reaction was determined by comparing the reactivity of tyrosine with its 3-nitro analog. The results imply that the electron transfer reaction is coupled to a proton transfer. The experimental conditions used in this model system provide a reasonable approximation to those involved in the radioprotection of DNA by tightly bound proteins in chromatin.

Introduction

The DNA damage by ionizing radiation is produced by two distinct routes.[1] These are the direct and the indirect effects. The direct effect refers to ionization by the radiation of the DNA itself. The indirect effect involves ionization of the solvent water, and intermediates derived from water radiolysis react with the DNA. These two routes can be distinguished since the reactive intermediates responsible for the indirect effect (mainly the hydroxyl radical, $^{\bullet}$OH) can be intercepted by intentionally added scavengers (for example glycerol or DMSO) to produce unreactive products.

In biological systems, the direct effect makes a *ca.* 30% contribution to the lethal effects of ionizing radiation.[2] This value far exceeds the fraction of ionizations that take place in the DNA and it is assumed to derive from the extensive scavenging that takes place in the highly concentrated conditions that exist in cellular nuclei and which therefore strongly attenuate the indirect effect.

Experimental systems that seek to model the direct effect must also decrease in some fashion the contribution of the otherwise dominant indirect effect. Examples include the use of high concentrations of scavengers, cryogenic temperatures, and dehydration.[3,4] These methods operate by respectively intercepting the reactive intermediates, preventing their diffusion, and preventing their formation. However there are artifacts associated with all of them. The use of scavengers can lead to the formation of reactive secondary radical products while freezing and dehydration unavoidably decrease the reactivity of DNA radical species with both water and oxygen. These rapid reactions are generally very important in aqueous radical chemistry.[1,5] In consequence our understanding of DNA damage by the direct effect is poor in comparison to that of the indirect effect.

Therefore the development of additional model systems is desirable, and the use of condensed DNA offers one possibility. Under mild conditions that include room temperature aqueous solutions of physiological ionic strength, binding of small cationic ligands to DNA brings about a large reduction in volume and an aggregation of multiple DNA molecules into compact particles with sizes in the micron range with packing densities comparable to those of chromatin.[6] DNA condensed in this fashion is extensively shielded from the bulk of the solution with the result that the indirect effect is extensively attenuated.[7,8]

Electron removal from DNA by the direct effect of ionizing radiation leaves radical cations which tend to migrate to guanine bases, because this represents the most stable location. DNA binding proteins may modulate the subsequent redox reactivity of these electron deficient species by electron transfer reactions from some amino acid residues. Electron donation by tyrosine is thermodynamically favorable, and has been observed from ligands bound to DNA. To further characterize the mechanism of this reaction, we report here the effect of changing its driving force by comparing the reactivity of tyrosine with its 3-nitro derivative.

Results and discussion

Reaction scheme

The scheme in Fig. 1 summarizes the important reactions involved in the modification of guanine residues when DNA is gamma-irradiated in aqueous solution. Details can be found in recent reviews.[5,9,10] Briefly, water radiolysis produces the hydroxyl radical $^{\bullet}$OH (reaction 1). Some $^{\bullet}$OH react with DNA to oxidize ribose

Department of Radiology, University of California at San Diego, 9500 Gilman Drive, La Jolla, CA 92093-0610, USA. E-mail: jmilligan@ucsd.edu; Fax: +1 858-534-0265; Tel: +1 858-534-4916

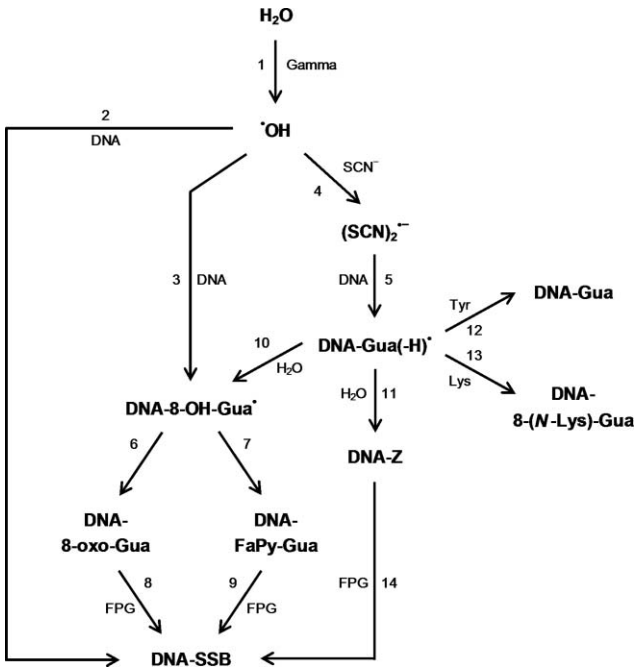

Fig. 1 Reaction scheme summarizing the most important reactions taking place in the formation of oxidative guanine (Gua) damage when aqueous plasmid DNA is gamma-irradiated in the presence of thiocyanate (SCN^-) and a derivative of tyrosine (Tyr) or lysine (Lys), and subsequently incubated with the enzyme FPG.

groups (reaction 2) and add to guanine (reaction 3), but in the presence of excess thiocyanate ions most are scavenged to produce the species $(SCN)_2^{\bullet-}$ (reaction 4). The species $(SCN)_2^{\bullet-}$ behaves as a mild single electron oxidizing agent which is capable of oxidizing only the guanine residues in DNA to produce (reaction 5) the DNA guanyl radical DNA-Gua(-H)•.[11] This guanine radical species is fairly stable with a lifetime on the order of seconds. It is trapped by water mainly at the C-8 position to produce (reaction 10) the radical species 8-hydroxy-7,8-dihydroguan-7-yl, DNA-8-OH-Gua•. This important reaction may be poorly modeled by experimental systems that employ extensive dehydration as a means to study the direct effect. The 8-hydroxylated radical gives rise to the two stable products 8-oxo-7,8-dihydroguanine, DNA-8-oxo-Gua (reaction 6) and 2,6-diamino-4-hydroxy-5-formamidopyrimidine, DNA-FaPy-Gua (reaction 7). Formation of a minor oxazolone product DNA-Z from the guanyl radical (reaction 11) has also been reported. All these water trapping products are converted to DNA single strand break (DNA-SSB) products by a post-irradiation incubation with the enzyme FPG (reactions 8, 9 and 14). Strand breaks convert the supercoiled conformation of the plasmid to its relaxed open circle form. This permits their yields to be quantified experimentally at the level of one per plasmid, equivalent to 10^{-1} pmole.

If a reducing agent such as tyrosine (Tyr) is present during irradiation, trapping of the guanyl radical by water (reaction 10, 11) is in competition with electron donation to the guanyl radical (reaction 12).[12] The effect of this electron transfer reaction is to reverse the oxidation of guanine and thus to repair the oxidative damage before it can be trapped as a stable product. The decrease in guanine oxidation can be quantified by the decrease in yield of FPG induced strand breaks. If a nucleophile such as lysine (Lys) is present during irradiation, it may replace water in trapping the guanyl radical (reaction 13). The product of this reaction is a crosslink between the C-8 position of guanine and the ε-amino group of lysine, DNA-(N^{ε}-Lys)-Gua.[13] With the tetralysine ligands we use here, the yield of this crosslinking reaction appears to be at least 10-fold smaller than the trapping reaction by water.[8]

An example of the formation of guanine oxidation products is shown in Fig. 2. Buffered aerobic aqueous solutions of plasmid DNA were gamma-irradiated in the presence of thiocyanate ions and the tyrosine derivative AcTyrOEt (the ethyl ester of *N*-acetyl tyrosine). After irradiation the plasmid was incubated with FPG. The formation of SSBs in the plasmid converts the supercoiled (SSB free) form into the open circle conformation. The decrease in the fraction of the supercoiled form is plotted in Fig. 2 against the radiation dose. Post-irradiation incubation with FPG results in a substantial decrease in the supercoiled form as oxidized guanine residues are converted to SSBs. The presence during irradiation of small levels of the tyrosine derivative attenuated this effect of FPG. The slopes of the yield dose plots in Fig. 2 can be interpreted directly in terms of the radiation chemical yield of the SSB products. By reference to Fig. 1, they can further be interpreted as yields of guanine oxidation products.

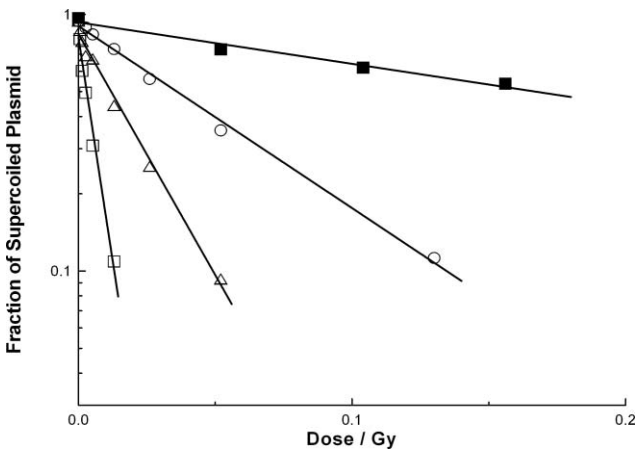

Fig. 2 Loss of supercoiled plasmid pHAZE due to gamma-irradiation. The plasmid was gamma-irradiated to the doses indicated under the conditions listed in the Materials and methods section. The tyrosine derivative present during irradiation was *N*-acetyltyrosine ethyl ester (AcTyrOEt) at a concentration of 1.0×10^{-6} mol L^{-1} (square), 3.0×10^{-6} mol L^{-1} (triangle), or 1.0×10^{-5} mol L^{-1} (circle). After irradiation and neutralization, the aliquots were incubated with (open symbols) or without (closed symbols) FPG and assayed electrophoretically. The fractions of the plasmid in the supercoiled conformation are plotted against the gamma-radiation dose. All four data sets are plotted on the same scale so that doses in the range 0.2 to 2.0 Gy have been omitted for clarity. Each data set is fitted with a least mean square straight line of the form $y = ae^{-mx}$. From the slopes m of these fitted lines, the D_0 doses are and the SSB yields for the four irradiation and incubation conditions are: 4.81×10^{-3} Gy and 3.01×10^{-2} μmol J^{-1} (open square); 1.07×10^{-2} Gy and 1.4×10^{-2} μmol J^{-1} (triangle); 5.33×10^{-2} Gy and 2.80×10^{-3} μmol J^{-1} (circle); 0.245 Gy and 6.07×10^{-4} μmol J^{-1} (closed square).

Kinetics of repair by monomeric tyrosine

Fig. 3 shows an example of the decrease in the yield of guanine oxidation in the presence of the tyrosine derivative AcTyrOEt and its

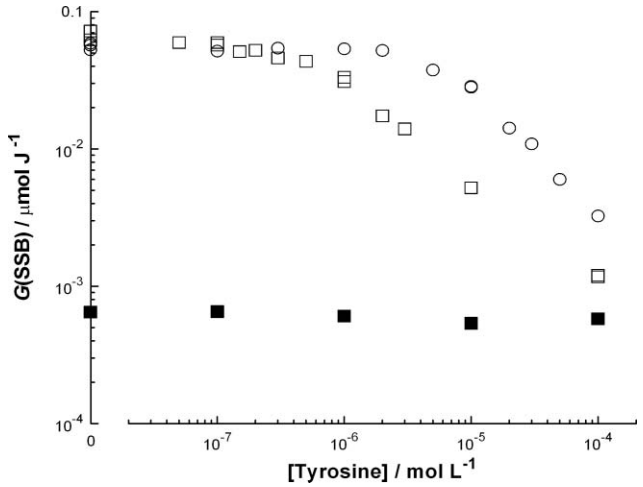

Fig. 3 Effect of the presence during irradiation of the tyrosine derivative AcTyrOEt (square) or Ac(NO_2Tyr)OEt (circle) on the SSB yield after incubation in the presence (open symbol) or absence (closed symbol) of FPG. Closed circle symbols are omitted for clarity. The SSB yields were quantified using the method shown in Fig. 2. The tyrosine derivative was present during gamma-irradiation at the concentration indicated on the X-axis.

3-nitro analog. The SSB yield was determined for many different concentrations of AcTyrOEt in the range 10^{-7} to 10^{-4} mol L^{-1}. The SSB yields (symbolized as G(SSB)) are plotted against the concentration of AcTyrOEt (and also of its 3-nitro analog) in Fig. 3. In the absence of any FPG incubation, the tyrosine derivative has no effect and the SSB yield remains constant at 6×10^{-4} μmol J^{-1}. This represents the minor formation of SSBs by $^{\bullet}$OH (reaction 2). After FPG incubation, SSBs are formed in larger yields that depend on the tyrosine concentration. This SSB yield is largest when no tyrosine is present, decreasing 70-fold from a value of 7×10^{-2} μmol J^{-1} (no added AcTyrOEt) to 1×10^{-3} μmol J^{-1} (10^{-4} mol L^{-1} AcTyrOEt). The 3-nitro analog has a smaller effect than its parent tyrosine.

The substrate specificity of FPG argues that this observation of a decrease in SSB yields can be interpreted in terms of an increasing attenuation of guanine oxidation.[14] In terms of the scheme in Fig. 1, this is further interpreted as an increase in the proportion of the DNA guanyl radical DNA-Gua(-H)$^{\bullet}$ undergoing reduction by tyrosine (reaction 12) to restore undamaged guanine (*i.e.*, to repair the guanine damage) with a corresponding decrease in the proportion being trapped by water (mainly reaction 10).

This competition between water and tyrosine for DNA-Gua(-H)$^{\bullet}$ can be interpreted quantitatively by application of conventional competition kinetics (eqn (1)).

$$\frac{1}{G(FPG)} = \left\{\frac{1}{G_0(FPG)}\right\} \times \left\{1 + \frac{k_{12}[Tyr]}{k_{10}}\right\} \quad (1)$$

The yield of sites recognized by FPG (G(FPG)) is defined as the SSB yield observed after incubation with FPG minus that observed without FPG. In the absence of any added tyrosine this yield is G_0(FPG). The rate constants for reactions 10 and 12 are respectively k_{10} and k_{12}. The linear dependence of G(FPG)$^{-1}$ on the concentration of the tyrosine derivative *Tyr* predicted by equation 1 is observed experimentally in the data sets for both AcTyrOEt and its 3-nitro analog from Fig. 3 (Fig. 4). From the slopes of the fitted straight lines, it can be concluded that the value of k_{12}/k_{10} is larger for AcTyrOEt than for its 3-nitro analog by a factor of $2.13 \times 10^7 / 1.98 \times 10^6 = 11$-fold. Although values are available for k_{10}, little is known of its pH dependence or of the effect of DNA condensation. Therefore we do not attempt to estimate absolute values for k_{12}, but prefer to leave the result as a relative form that quantified the factor by which AcTyrOEt reacts faster than its 3-nitro cognate.

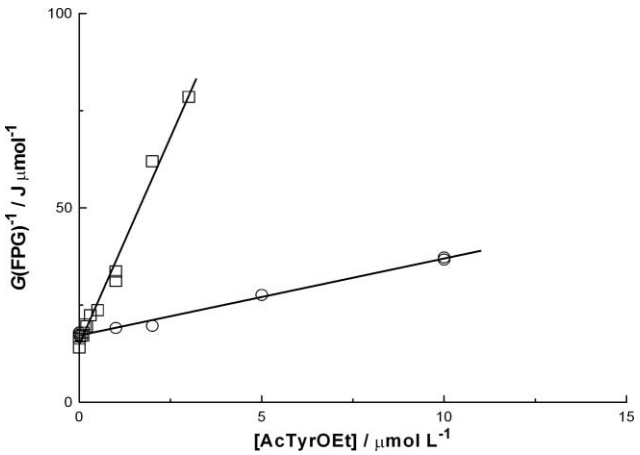

Fig. 4 Comparison of the reactivities of the tyrosine derivatives AcTyrOEt (square) or Ac(NO_2Tyr)OEt (circle). The reciprocal of the yield of sites recognized by the enzyme FPG (see text) is plotted according to competition kinetics against the concentration of the tyrosine derivative present during gamma-irradiation. The two data sets are fitted with least mean square straight lines of the form $y = mx + c$. The values of the slopes m are 2.13×10^7 MJ L mol^{-2} (square) and 1.98×10^6 MJ L mol^{-2} (circle).

Effect of cationic tyrosine derivatives

We have reported previously that cationic oligolysine ligands are able to condense plasmid DNA into compact particles with sizes in the micron range.[8,15] The conditions required for the three ligands Lys_2-Tyr-Lys_2, its 3-nitro analog Lys_2-(NO_2)Tyr-Lys_2, and its tyrosine free parent Lys_4 (tetralysine) to condense DNA are all very similar (not shown) implying that the binding constants and their ionic strength dependencies are all also very similar.[16] DNA packing in such particles is comparable to that of chromatin.[6] The decrease in exposure to the bulk of the solvent results in an extensive protection against the indirect effect (attack by water radicals) and provides a means to examine DNA damage by the direct effect (ionization of the DNA itself) under conditions where water is still present. If some of the ligands additionally carry tyrosine residues, we can use such a system to examine the competition between reactions 10 and 12 under conditions where the DNA is highly compacted, well hydrated, and in close contact with a tyrosine residue. We argue that this represents a better approximation to mammalian chromatin than other model systems for the direct effect.

The attenuation of guanine oxidation shown in Fig. 3 and 4 for the monomeric tyrosine compounds AcTyrOEt (and its 3-nitro analog) was repeated using the cationic ligand Lys_2-Tyr-Lys_2 (and its 3-nitro analog) using two different ionic conditions (the redox inactive parent ligand Lys_4 was also present such that the total ligand concentration was 5×10^{-4} mol L^{-1}).

At a high ionic strength (in the presence of 3.5×10^{-2} mol L^{-1} sodium perchlorate), electrostatic binding of the ligands is decreased and the plasmid remains uncondensed, although the radiation chemistry of the solution is unaffected.[8] Observations made under these conditions (not shown) were very similar to those in Fig. 3 and 4, and the factor by which k_{12}/k_{10} for Lys_2-Tyr-Lys_2 exceeds that for its 3-nitro analog is found to be $8.12 \times 10^8/6.34 \times 10^7 = 13$-fold. This comparison was repeated in the absence of added sodium perchlorate where the total ligand concentration of 5×10^{-4} mol L^{-1} (contributed mostly by the redox inactive ligand Lys_4) was sufficient to condense the plasmid. SSB yields are about 50-fold lower under these conditions because of the protection against the indirect effect. But attenuation of guanine oxidation by tyrosines is still clearly observed (Fig. 5). Simple competition kinetics fails with condensed DNA, but the difference in reactivity between Lys_2-Tyr-Lys_2 and its 3-nitro analog Lys_2-(NO_2)Tyr-Lys_2 can still be quantified by determining the horizontal displacement between the two data sets in Fig. 5. The ratio is approximately 7-fold.

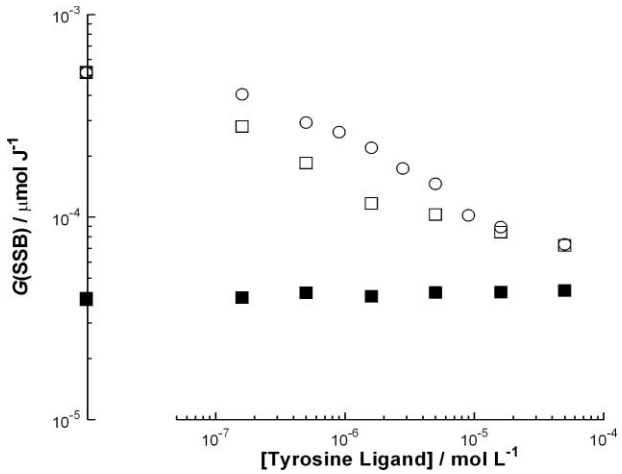

Fig. 5 Effect of the presence during irradiation of the ligands Lys_2-Tyr-Lys_2 (square) and Lys_2-(NO_2Tyr)-Lys_2 (circle) under condensed conditions (see text) on the SSB yield after incubation in the presence (open symbol) or absence (closed symbol) of FPG. Closed circle symbols are omitted for clarity. The parent ligand Lys_4 was also present during irradiation such that the total ligand concentration was 5×10^{-4} mol L^{-1}. SSB yields were determined using the method of Fig. 2.

Given the complexities of this non-homogeneous model system and the uncertainties inherent in the estimation of the SSB yields, the three estimates of the difference of reactivity of tyrosine and 3-nitrotyrosine of 11-fold, 13-fold, and 7-fold compare reasonably favorably with one another.

Thermodynamics of repair

We wish to compare the reactivity differences between tyrosine and 3-nitrotyrosine we have quantified here with previous measurements made using structurally similar phenols (for which far more extensive thermodynamic data is available) in order to characterize the mechanism of the electron transfer reaction.[17] To do so requires the assumption that redox data for the monomeric tyrosine AcTyrOEt (and for its 3-nitro analog) are applicable to the tetralysine ligands Lys_2-Tyr-Lys_2 and Lys_2-(NO_2)Tyr-Lys_2.

Table 1 Acidity data for guanine and tyrosine derivatives

Acid		Base	pK_a	Citation
$Gua^{\bullet+}$	⇆	$Gua(-H)^{\bullet}$	3.9	24, 25
Gua	⇆	$Gua(-H)^{-}$	9.5	25
Ac(TyrOH)OEt	⇆	Ac($TyrO^{-}$)OEt	10.0	this work
Ac(NO_2TyrOH)OEt	⇆	Ac(NO_2TyrO^{-})OEt	7.2	"
Lys_2-(TyrOH)-Lys_2	⇆	Lys_2-($TyrO^{-}$)-Lys_2	9.8	"
Lys_2-(NO_2TyrOH)-Lys_2	⇆	Lys_2-(NO_2TyrO^{-})-Lys_2	6.4	"
4-CH_3-C_6H_4-$OH^{\bullet+}$	⇆	4-CH_3-C_6H_4-$O^{\bullet}$	-1.6	18
2-NO_2-C_6H_4-$OH^{\bullet+}$	⇆	2-NO_2-C_6H_4-$O^{\bullet}$	-2.0	18

Table 2 Literature reduction potential data for guanine and tyrosine derivatives

Couple	E/V	Citation
$Gua(-H)^{\bullet}$, H^+/Gua	+1.29	(pH 7) 20
Ac($TyrO^{\bullet}$)NH_2/Ac($TyrO^{-}$)NH_2	+0.64	19
Ac($NO_2TyrO^{\bullet}$)NH_2/Ac(NO_2TyrO^{-})NH_2	+1.00	19

Using spectrophotometric titration (not shown), we determined the pK_a values for these four tyrosine containing compounds. The results are listed in Table 1 together with literature acidity data for guanine and phenol derivatives. The acidities of the radical cations of *p*-cresol and 2-nitrophenol are assumed to apply to AcTyrOEt and to its 3-nitro analog respectively. This assumption seems reasonable since the pK_a values of many phenolic radical cations lie in the range of –1 or –2.[18]

Reduction potential data are available for the carboxylic acid amide of *N*-acetyltyrosine and its 3-nitro analog from pH 3 to 12 (Table 2).[19] They are assumed to apply to AcTyrOEt and its 3-nitro analog. This is supported by the close similarity in acidity of the phenolic OH groups in these compounds. Table 2 also contains literature reduction potential data for guanosine,[20] which is assumed to apply to guanine bases in plasmid DNA.[21]

Because of acidity differences between the guanyl radical and tyrosine, the reduction of the former by the latter (reaction 12) involves the transfer of a proton as well as of an electron. Under the reaction conditions, the reactants are $Gua(-H)^{\bullet}$ and TyrOH while the products are Gua and $TyrO^{\bullet}$. The individual proton and electron transfers are symbolized in the reaction scheme of Fig. 6 where the resulting intermediates are all identified. For example, transferring the electron from tyrosine to guanine (reaction 12A) before the proton (reaction 12B) produces the intermediates $Gua(-H)^{-}$ and $TyrOH^{\bullet+}$. It is also possible that the electron and proton are both transferred on the same time scale (reaction 12C), a reaction described as a proton coupled electron transfer. The derived reduction potential data for the species involved are listed in Table 3, so that it is possible to calculate the reduction potentials ΔE (and therefore driving forces ΔG) for the three electron transfer steps in Fig. 6. The ΔG values for the proton transfer steps can be calculated from the acidity differences or from the thermodynamic cycles in Fig. 6. The results are listed in Table 4 for both AcTyrOEt and its 3-nitro analog.

The acidities of the phenolic groups are less than 1 pK_a unit lower in the tetralysine ligands than in the monomers (Table 1), and so we assume that the reduction potential data for the monomers provide an equally reliable estimate for the ligands. This is equivalent to an error of 5 kJ mol^{-1} in the ΔG values listed in Table 4. The largest sources of uncertainty in these values

Table 3 Derived reduction potential data for guanine and tyrosine derivatives

Couple	E/V	pH range
Gua(-H)$^{\bullet}$, H$^+$/Gua	+1.38	pH = 5.5
Gua$^{\bullet+}$/Gua	+1.47	pH < 3.9
Gua(-H)$^{\bullet}$/Gua(-H)$^-$	+1.14	pH > 9.5
Ac(TyrO$^{\bullet}$)OEt, H$^+$/Ac(TyrOH)OEt	+0.90	pH = 5.5
Ac(TyrOH$^{\bullet+}$)OEt/Ac(TyrOH)OEt	+1.32	pH < –1.6
Ac(TyrO$^{\bullet}$)OEt/Ac(TyrO$^-$)OEt	+0.64	pH > 10.0
Ac(NO$_2$TyrO$^{\bullet}$)OEt, H$^+$/Ac(NO$_2$TyrOH)OEt	+1.09	pH = 5.5
Ac(NO$_2$TyrOH$^{\bullet+}$)OEt/Ac(NO$_2$TyrOH)OEt	+1.53	pH < –2.0
Ac(NO$_2$TyrO$^{\bullet}$)OEt/Ac(NO$_2$TyrO$^-$)OEt	+1.00	pH > 7.2

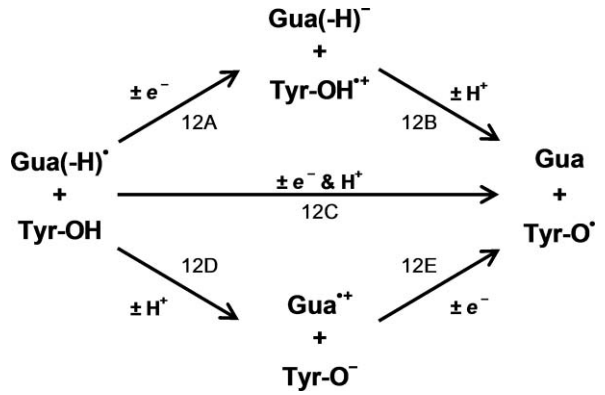

Fig. 6 Reaction scheme depicting the individual proton and electron transfer reactions that are involved in the reduction of a DNA guanyl radical by a tyrosine derivative (reaction 12 in Fig. 1). The phenolic OH group is assumed to act as the proton source. The three pathways are electron before proton (reactions 12A and 12B); proton coupled electron transfer (reaction 12C); and proton before electron (reactions 12D and 12E).

would probably be the effect of DNA base sequence on the guanyl radical reduction potentials and on acid dissociation constants of up to 0.08 V[22] and 1.6 pK_a units.[23] These are equivalent to 8 and 9 kJ mol^{-1}. However these uncertainties in absolute values are mitigated by our consistent use of the same DNA target in all cases. The ΔG values in Table 4 are assumed to be applicable to all three experimental measurements of the difference in reactivity of tyrosine and 3-nitrotyrosine: (1) monomers; (2) ligands with uncondensed plasmid (high ionic strength); and (3) ligands with condensed plasmid (low ionic strength).

Comparison of kinetics with thermodynamics

The likelihood of the three different electron transfer steps in Fig. 6 can be assessed by comparing the estimates for their driving forces with the experimental observations for the difference in reactivity between tyrosine and 3-nitrotyrosine. Marcus theory describes the relationship between them in quantitative terms as $\log_e k = C - (\Delta G + \lambda)^2/4\lambda RT$, where k is the rate constant, C an arbitrary constant, and λ the reorganization energy.[26] It is difficult to determine λ in this system, and as discussed above we do not possess absolute values for k_{12}, only for the ratio k_{12}/k_{10}. Therefore an indirect approach is necessary, which has been applied by others.[27]

Table 4 Driving forces for individual proton and electron transfers in Fig. 6

	ΔG/kJ mol^{-1}				
Tyrosine derivative	12A	12B	12C	12D	12E
AcTyrOEt	+17	–63	–46	+34	–80
Ac(NO$_2$Tyr)OEt	+38	–66	–28	+19	–45

The relationship between k and ΔG can be expressed in differential form as $\partial(RT\log_e k)/\partial\Delta G = -(\frac{1}{2} + \Delta G/2\lambda)$. So even if λ is unknown and k known only in relative terms, it is still possible to conclude that the plot of $RT\log_e k$ against ΔG should have a negative slope whose magnitude is less steep than $\frac{1}{2}$ if ΔG is negative and more steep than $\frac{1}{2}$ if ΔG is positive. The vertical displacement of $RT\log_e k$ is calculated from the ratios of 11-fold, 13-fold, and 7-fold as 5.9, 6.4, and 4.8 kJ mol^{-1} respectively. These values are plotted against the ΔG values for reaction 12C (from Table 4) in Fig. 7 along with data for eight different mono-substituted phenols which we have reported previously.[17] Recall that the absolute Y-values of the lines in Fig. 7 are undefined and that the purpose is to compare only the *slopes* of the straight lines (of –0.2, –0.3, and –0.1 representing respectively the 11-, 13-, and 7-fold ratios observed with the tyrosines) with the *trend* of the symbols representing observations with simple phenols.

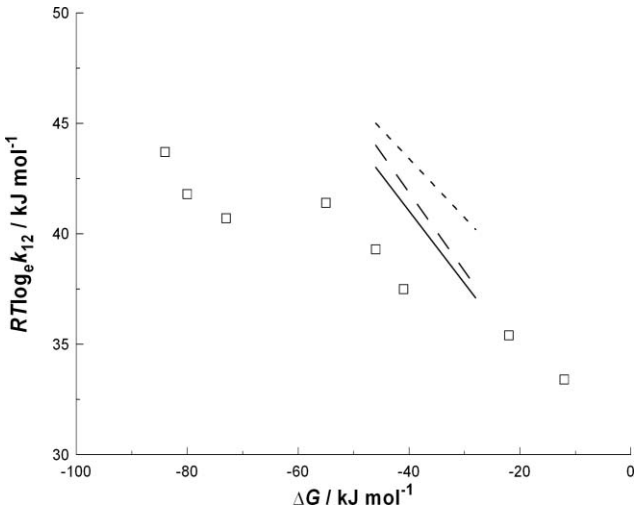

Fig. 7 Comparison between the observed rate constant for electron transfer from tyrosine to a guanyl radical (reaction 12) with the calculated driving force for the reaction according to the Marcus theory (see text). The three ratios of $k_{12}/k_{10} = 11$ (solid line), 13 (long dash), and 7 (short dash) respectively are plotted in terms of $RT\log_e(k_{12}/k_{10})$ against the driving forces for reaction 12C listed in Table 4. The absolute Y-values are arbitrary and only the slopes are of importance. Previously reported data for phenols (squares) are included for comparison.

Reaction 12A (electron before proton) involves large positive values for ΔG, and a slope of magnitude less steep than $-\frac{1}{2}$ is inconsistent with the Marcus theory. We have argued previously that reaction 12E (electron after proton) requires a preceding and highly unfavorable proton transfer that in the same system (although at a higher pH value) is very probably slower than the observed absolute rate constant. Therefore the previous conclusion that the repair of guanyl radicals in DNA by simple phenols involves a proton coupled electron transfer[17] appears also to be valid in DNA condensed with a tyrosine containing ligand. As described in the introduction, we argue that the use of DNA

condensed with a cationic ligand provides a superior model for the behavior of tyrosine residues in DNA binding proteins or in chromatin.

Conclusions

We describe a plasmid DNA model in which oxidative DNA damage can be reversed by electron donation from tyrosine. In three closely related systems, the 3-nitro derivative of tyrosine is less reactive than its parent by 7- to 13-fold. A comparison of the kinetics and thermodynamics of this reaction suggests that the mechanism of the reaction involves a proton coupled electron transfer.

Experimental

Biochemical reagents

Plasmid pHAZE[28] was grown to a large scale in an *E. coli* host. Its isolation and purification have been described previously.[14] The base excision repair endonuclease formamidopyrimidine-DNA *N*-glycosylase (FPG protein) was obtained from Trevigen (Gaitherburg, MD). Tetralysine peptides were obtained from Biomatik (Wilmington, DE).

Spectrophotometric titration

Phenolic pK_a values were determined spectrophotometrically at the ionic conditions used in the irradiation (6.0×10^{-2} mol L^{-1} sodium ion concentration, not shown). The values are listed in Table 1.

Condensation threshold

The change in radiosensitivity associated with DNA condensation was determined by gamma-irradiation in the buffer system described below, but replacing sodium thiocyanate with glycerol. The presence of glycerol ensures a relatively constant $^{\bullet}OH$ scavenging capacity despite the change in tyrosine concentration.

Radioprotection by tyrosines

Aerobic solutions of plasmid pHAZE (size 1.03×10^4 base pairs[28]) were gamma-irradiated with an AECL Gamma Cell 1000 instrument (^{137}Cs isotope, 662 keV photon). The dose rate of 311 rad min^{-1} was measured by using the Fricke system.[29] The solution (7 μL aliquot) contained plasmid pHAZE (100 μg mL^{-1}), equivalent to 3.1×10^{-4} mol L^{-1} nucleotide residues or 1.5×10^{-8} mol L^{-1} plasmid), sodium hydrogen phosphate (6.0×10^{-2} mol L^{-1}), disodium hydrogen phosphate (2.0×10^{-3} mol L^{-1}), sodium perchlorate (zero to 3.5×10^{-2} mol L^{-1}), sodium thiocyanate (1×10^{-3} mol L^{-1}), a tyrosine derivative (zero to 10^{-4} mol L^{-1}), and tetralysine (zero to 5×10^{-4} mol L^{-1}). The relatively acidic conditions (pH 5.6) were chosen to ensure that the nitrotyrosine phenolic OH group was largely protonated (Table 1). The tyrosine derivative was one of four compounds: *N*-acetyltyrosine ethyl ester, AcTyrOEt; *N*-acetyl-3-nitrotyrosine ethyl ester, Ac(NO_2Tyr)OEt; lysyl-lysyl-tyrosyl-lysyl-lysine, Lys_2-Tyr-Lys_2; and lysyl-lysyl-3-nitrotyrosyl-lysyl-lysine, Lys_2-(NO_2Tyr)-Lys_2. We use "tyrosine" to refer to any or all of these compounds, not to the parent amino acid itself. After irradiation the samples were mixed with a solution (20 μL) containing sodium phosphate buffer components such that the buffer ratio was brought to 1 : 1 and the total sodium ion concentration was 0.12 mol L^{-1}. The purpose was to adjust the pH and ionic composition of the solution so that they became compatible with the requirements of the enzyme FPG[14] and that the ionic strength was sufficiently large to reverse any DNA condensation (if applicable).

FPG incubation

After irradiation and subsequent dilution, the resulting solutions were treated with FPG (3 μL) such that its final concentration was either zero or 3 μg mL^{-1} (either zero or 30 units mL^{-1}). They were then incubated at 37 °C for 30 min. These conditions represent an excess of FPG.[11]

Strand break yield

After incubation, the plasmid was assayed for strand breaks by agarose gel electrophoresis. We have reported previously on the method of digital video imaging of ethidium fluorescence to quantify the yield of single strand breaks (SSB) in the plasmid target.[30] Briefly, the D_0 gamma radiation dose (the dose required to reduce the fraction of SSB-free plasmid by a factor of *e*, which assuming a Poisson distribution is equivalent to producing a mean of one SSB per plasmid) is equal to the reciprocal of the slope *m* of a straight line fitted to a semi logarithmic yield-dose plot. At the D_0 dose, the concentration of the SSB product is equal to the concentration of the plasmid (1.5×10^{-8} mol L^{-1}, see above). The radiation chemical yield or *G*-value (units of mol J^{-1}) is calculated by dividing this concentration by the value of D_0.

Acknowledgements

Supported by PHS grant CA46295.

References

1 C. von Sonntag. *The chemical basis of radiation biology*, Taylor and Francis, Philadephia, 1987.
2 J. D. Chapman, A. P. Reuvers, J. Borsa and C. L. Greenstock, *Radiat. Res.*, 1973, **56**, 291–306.
3 S. G. Swarts, D. Becker, M. Sevilla and K. T. Wheeler, *Radiat. Res.*, 1996, **145**, 304–314.
4 Y. Razskazovskiy, M. G. Debije and W. A. Bernhard, *Radiat. Res.*, 2003, **159**, 663–669.
5 W. K. Pogozelski and T. D. Tullius, *Chem. Rev.*, 1998, **98**, 1089–1108.
6 S. He, P. G. Arscott and V. A. Bloomfield, *Biopolymers*, 2000, **53**, 329–341.
7 G. L. Newton, J. A. Aguilera, J. F. Ward and R. C. Fahey, *Radiat. Res.*, 1996, **145**, 776–780.
8 A. Ly, S. Bullick, J.-H. Won and J. R. Milligan, *Int. J. Radiat. Biol.*, 2006, **82**, 421–433.
9 J. Cadet, T. Douki and J.-L. Ravanat, *Acc. Chem. Res.*, 2008, **41**, 1075–1083.
10 C. J. Burrows and J. G. Muller, *Chem. Rev.*, 1998, **98**, 1109–1152.
11 J. R. Milligan, J. A. Aguilera, R. A. Paglinawan and J. F. Ward, *Int. J. Radiat. Biol.*, 2000, **76**, 1305–1314.
12 J. R. Milligan, N. Q. Tran, A. Ly and J. F. Ward, *Biochemistry*, 2004, **43**, 5102–5108.
13 S. Perrier, J. Hau, D. Gasparutto, J. Cadet, A. Favier and J.-L. Ravanat, *J. Am. Chem. Soc.*, 2006, **128**, 5703–5710.
14 J. T. Stivers and Y. L. Yang, *Chem. Rev.*, 2003, **103**, 2729–2759.
15 I. Nayvelt, T. Thomas and T. J. Thomas, *Biomacromolecules*, 2007, **8**, 477–484.

16 D. P. Mascotti and T. M. Lohman, *Proc. Natl. Acad. Sci. U. S. A.*, 1990, **87**, 3142–3146.
17 J. R. Milligan, J. A. Aguilera, O. Hoang, A. Ly, N. Q. Tran and J. F. Ward, *J. Am. Chem. Soc.*, 2004, **126**, 1682–1687.
18 D. M. Holton and D. Murphy, *J. Chem. Soc., Faraday Trans. 2*, 1979, **75**, 1637–1642.
19 C. S. Yee, M. R. Seyedsayamdost, M. C. Chang, D. G. Nocera and J. Stubbe, *Biochemistry*, 2003, **42**, 14541–14552.
20 S. Steenken and S. V. Jovanovic, *J. Am. Chem. Soc.*, 1997, **119**, 617–618.
21 S. S. Shinde, A. Maroz, M. P. Hay and R. F. Anderson, *J. Am. Chem. Soc.*, 2009, **131**, 5203–5207.
22 F. D. Lewis, X. Liu, J. Liu, R. T. Hayes and M. R. Wasielewski, *J. Am. Chem. Soc.*, 2000, **122**, 12037–12038.
23 S. Acharya, J. Barmann, P. Cheruku, S. Chatterjee, P. Acharya, J. Isaksson and J. Chattopadhyaya, *J. Am. Chem. Soc.*, 2004, **126**, 8674–8681.
24 L. P. Candeias and S. Steenken, *Chem.–Eur. J.*, 2000, **6**, 475–484.
25 S. Steenken, *Free Radical Res.*, 1992, **16**, 349–379.
26 R. A. Marcus and N. Sutin, *Biochim. Biophys. Acta*, 1985, **811**, 265–322.
27 M. S. Graige, M. L. Paddock, J. M. Bruce, G. Feher and M. Y. Okamura, *J. Am. Chem. Soc.*, 1996, **118**, 9005–9106.
28 L. H. Lutze and R. A. Winegar, *Mutat. Res. Lett.*, 1990, **245**, 305–310.
29 J. W. T. Spinks and R. J. Woods. *An introduction to radiation chemistry, 3rd edition*, Wiley, New York, 1990.
30 J. R. Milligan, J. A. Aguilera and J. F. Ward, *Radiat. Res.*, 1993, **133**, 151–157.